Available online at www.sciencedirect.com
SCIENCE DIRECT
Journal of Pharmaceutical and Biomedical Analysis 41 (2006) 1473–1478
JOURNAL OF PHARMACEUTICAL AND BIOMEDICAL ANALYSIS
www.elsevier.com/locate/jpba

Short communication

Effect of calcination cycles on the preparation of tin oxide based traditional drug: Studies on its formation and characterization

M.P. Wadekar [a], C.V. Rode [b,*], Y.N. Bendale [c], K.R. Patil [d], A.B. Gaikwad [d], A.A. Prabhune [a,**]

[a] *Division of Biochemical Sciences, National Chemical Laboratory, Pune 411008, India*
[b] *Homogeneous Catalysis Division, National Chemical Laboratory, Pune 411008, India*
[c] *Ayurved Rasayani, Sinhgad Road, Pune 411052, India*
[d] *Center for Material Characterization, National Chemical Laboratory, Pune 411008, India*

Received 22 February 2006; received in revised form 25 March 2006; accepted 29 March 2006
Available online 8 May 2006

Abstract

The preparation method of metal based Indian traditional drugs involves conversion of a pure metal into its oxide by repeated high temperature calcination cycles. In this work, the effect of number of calcination cycles followed in the preparation of tin oxide based Ayurvedic drug, 'vanga bhasma' was studied by a systematic characterization of the drug samples after various calcination stages. It was found that tin was in the form of Sn^{4+} state and that the formation of SnO_2 proceeded step-wise through $Sn(OH)_4$.

Keywords: Tin oxide; Vanga bhasma; Calcination cycles; Oxidation; Oxidation state of tin; Particle size

1. Introduction

The drugs known as 'bhasmas' are well known in the traditional Indian Ayurveda and these are chemically mixed oxides of one or more metals [1]. Their traditional preparation involves conversion of a pure metal into its oxide form following a typical procedure, available in the ancient literature of Ayurveda [2]. Such a procedure is believed to eliminate the harmful properties of metal oxides while inducing the medicinal properties into it. The critical steps in the preparation of 'bhasma' are: (i) trituration of a pure metal with various plant juices for several hours and (ii) repeated cycles of high temperature calcination in a sealed earthen pot. From the point of view of basic understanding and also to standardize such drugs it would be essential to carry out their structural characterization and also to study the role of various steps involved in the preparation protocol. As a continuation of our efforts in this direction, we report here the effect of repeated calcination cycles on the formation of 'vanga bhasma', viz. tin oxide which is among the seven Ayurvedic 'bhasmas' reported in the ancient literature. 'Vanga bhasma' is generally administered for various types of genito-urinary tract disorders [3]. It is also an effective medicine in various other diseases like diabetes, anaemia, asthama and gastric ulcers [4]. Based on the characterization of tin oxide at various stages of calcination, we propose a step-wise oxidation of tin going through its hydroxide formation. Further, the presence of calcium from the plant origin probably stabilizes the particle size of tin oxide inspite of repeated high temperature calcination cycles.

2. Experimental

For preparing 'vanga bhasma' tin wire (purity >99.99%) was subjected to the traditional ayurvedic pretreatment involving melting the tin wire (1 kg) and dipping it successively in oil of *sesamum indicum*, butter milk, cow urine and aqueous extract of dolochos seven times each. Finally, the molten tin was kept in contact with limewater for about 3 h.

For obtaining the required drug, the traditional calcination protocol called as 'bhasmikarna' was carried out. This involved mainly the trituration of the pretreated tin with powder of dried tamarind (*Tamarindus indica*) nut shells, bark of *Ficus religiosa* and *Curcuma longa*. The crude product was powdered and mixed with *Aloe vera* juice to obtain a homogeneous paste, which was

* Corresponding author. Tel.: +91 20 2590 2349; fax: +91 20 2589 2621.
** Co-corresponding author.
E-mail addresses: cv.rode@ncl.res.in (C.V. Rode), aa.prabhune@ncl.res.in (A.A. Prabhune).

0731-7085/$ – see front matter © 2006 Elsevier B.V. All rights reserved.
doi:10.1016/j.jpba.2006.03.032

Table 1
XRD crystallite sizes of the drug samples after various calcination stages

Sample name	2θ values at $I/I_0 = 100$	FWHM (radian)	d-Value	Crystallite size (nm)
SNB-1	33.9	0.329	2.640	25.26
SNB-7	34.1	0.353	2.627	23.56
SNB-13	34.2	0.353	2.616	23.56
SNB-15	34.1	0.353	2.625	23.56
SNB-17	33.8	0.329	2.645	25.26
SN-STD	33.9	0.306	2.639	27.17

transferred to the earthenware crucibles and sealed with the clay. The calcination was then carried out in the traditional furnace (temperature of 600 °C) following the procedure described by Pandit et al. [5]. After overnight calcinations, the product was taken out, the undesired ash was removed and the sample was named as (SNB-1). In this manner, 17 cycles of calcinations were carried out and the samples at the end of calcination cycles 1, 7, 13, 15 and 17 (designated as SNB-1, SNB-7, SNB-13, SNB-15 and SNB-17) were thoroughly characterized. The standard tin oxide was procured from Aldrich.

The XRD patterns of the solid samples were recorded on Regaku cd-max II vc model X-ray diffractometer using Cu Kα radiation filtered by a nickel foil over the range of diffraction 3–80°. The wavelength of the radiation was 1.5405 Å.

The chemical composition of the samples was determined by EDX attached to SEM (JEOL JSM 200). IR spectra in the region (4000–450 cm^{-1}) were recorded on Perkin-Elmer FTIR spectrophotometer in KBr pellets. Far IR spectra in the low frequency region (600–50 cm^{-1}) were recorded on Nexus-870 model (Nicolet). Thermograms were recorded in air atmosphere on NETZSCH simultaneous thermoanalyzer STA-409 model with Pt and Rh thermocouples.

XPS were recorded with a nine channeltron CLAM4 analyzer under a vacuum $>1 \times 10^{-8}$ Torr using Al Kα radiation

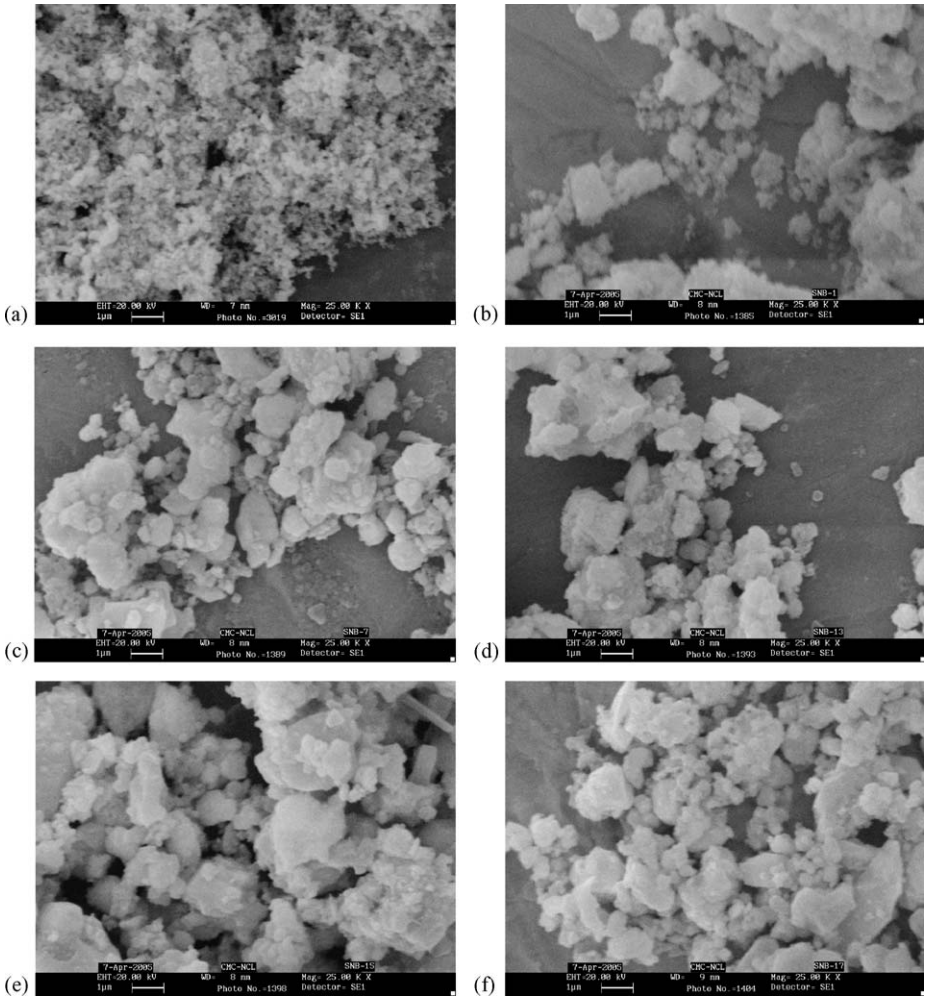

Fig. 1. SEM of standard tin oxide (a) and the drug samples after (b) 1st, (c) 7th, (d) 13th, (e) 15th and (f) 17th calcination cycles.

and constant pass energy of 50 eV. The binding energy values (accurate to ±0.2 eV) were charge-corrected to the C 1s signal (284.6 eV). BET surface area analysis was done using Chembet 3000 surface area analyzer of Quantachrome USA.

3. Results and discussion

3.1. XRD

XRD patterns of samples of different calcination cycles of 'vanga bhasma' showed 2θ values around 26.6, 34, 38.2, 39, 51.8, 54.8, 57.9, 61.9, 64.8° which were close to those reported for the standard tin (IV) oxide (tetragonal-rutile phase) diffraction peaks [6,7]. This indicated that in all stages of 'vanga bhasma', SnO_2 was the major constituent while the intense nature of peaks showed that at all calcination cycles the samples were of higher crystallinity. The crystallite sizes of tin oxide in the 'vanga bhasma' after various calcination cycles were calculated from XRD pattern (2θ for 100% intensity peaks) following the Scherrer Equation and were compared with that of the standard SnO_2 [8]. It was found that (Table 1) after the first calcination cycle, the crystallite size decreased from 25.26 to 23.56 nm, which remained constant during further calcination cycles however, it again increased to 25.26 nm after the 17th calcination cycle. The crystallite sizes of all the samples were anyway lower than that of the standard tin oxide (Table 1) which clearly showed that the size stabilization of the tin oxide crystallite in the drug sample was due to the presence of calcium from tamarind nut shells [9]. It has been already reported that calcium was responsible for size stabilization of SnO_2 [10].

3.2. SEM and EDX analysis

The photographs of SEM taken for the standard tin oxide (a) and the samples of the drug 'vanga bhasma' after different cycles of calcination (b–f) are shown in Fig. 1. It was found that (i) samples at different calcination cycles showed higher degree of agglomeration (particle size in the range of 2–5 μm) than that shown by standard SnO_2 sample in which the particle size was in the range of 0.1–0.5 μm. (ii) Morphology of 'vanga bhasma' samples was remarkably different from that of the standard SnO_2 however, in both the cases grain boundaries were not well defined. (iii) In case of SNB-1 (after first calcination cycle), spongy and relatively compact microcrystalline aggregates of SnO_2 were observed which were covered by small dusty crystallites (particle size of 1–2 μm). (iv) After several repeated calcination cycles (SNB-7 sample), spongy nature of the crystallites was retained while agglomeration increased as indicated by the increased particle size up to 5 μm. Extended cycles of calcination increased the extent of agglomeration as seen by more particles of 6 μm in SNB-13 sample. (v) A distinct change in the morphology occurred with further calcination cycles as several well-defined rod shaped particles were seen in the SEM of SNB-15. (vi) Surprisingly, at the end of 17th cycle of calcination (SNB-17 sample), extent of agglomeration was found to be reduced as evidenced by more particles of 1 μm size. Also higher number of smaller agglomerates was observed in SEM of SNB-17, which indicates that beyond 15 cycles of calcination bigger agglomerates start disintegrating to give a stable particle size of 1 μm. Thus, repeated calcination cycles are necessary for not only achieving higher conversion of metallic tin to tin oxide but also to stabilize the particles to a minimum of 1 μm.

The elemental composition of samples after various stages of calcination of the drug, 'vanga bhasma' by EDX is presented in Table 2. Relative percentage of Sn increased from 50 to 59% with increase in calcination cycles. The maximum Sn content in the standard tin oxide was 78% while that in the SNB-17 drug sample was 59% which was equivalent to 75.77% SnO_2 (as per the stoichiometry). The remaining major element was stoichiometric excess oxygen due to the repeated calcination procedure followed in the preparation of this drug sample [1]. Elements, such as Mg, Si, Ca and Fe were also found to be present, mainly introduced from the plant material used during the trituration process. Presence of calcium in all samples was important since it inhibits the crystallite growth of tin oxide [10].

3.3. XPS

XPS analysis was carried out for three important stages of 'vanga bhasma' namely SNB-1, SNB-7 and SNB-17. Fig. 2 shows a typical survey spectrum of SNB-1 sample, confirming the presence of Sn and Ca. In addition, it also shows the presence of C peak as well as O peak at 284.6 and 531 eV, respectively as impurities. Although the presence of Mg and Fe was shown in EDX analysis, these ions were not observed in XPS analysis, indicating their absence on the surface. In all the three samples (Fig. 3(a)), high resolution spectra at Sn-core level showed the presence of strong peaks at 486.5 and 494.8 eV corresponding to Sn $3d_{5/2}$ and Sn $3d_{3/2}$, respectively, for SnO_2 phase [11,12]. The position of the peaks for SnO and $Sn(OH)_4$ were very close to each other and therefore could not be resolved, as observed

Table 2
EDX analysis of the 'vanga bhasma' at various calcination stages

Sample name	C	O	Mg	Si	Fe	Ca	Sn	SnO_2
Sn-STD	–	21.24	–	–	–	–	78.76	100
SNB-1	5.98	30.61	2.42	4.90	3.61	3.11	50.36	63.94
SNB-7	5.46	29.08	1.29	3.59	2.05	1.97	56.56	71.81
SNB-13	4.53	31.19	1.26	4.43	2.53	2.32	53.74	68.23
SNB-15	2.44	29.35	1.36	5.06	2.25	2.62	56.91	72.26
SNB-17	1.63	23.86	1.70	3.91	2.46	1.75	59.68	75.77

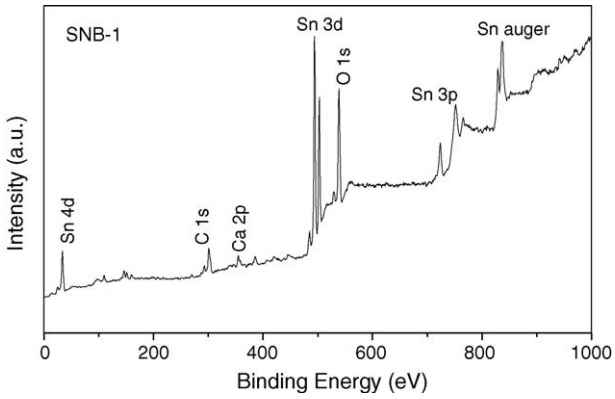

Fig. 2. XPS of the sample SNB-1.

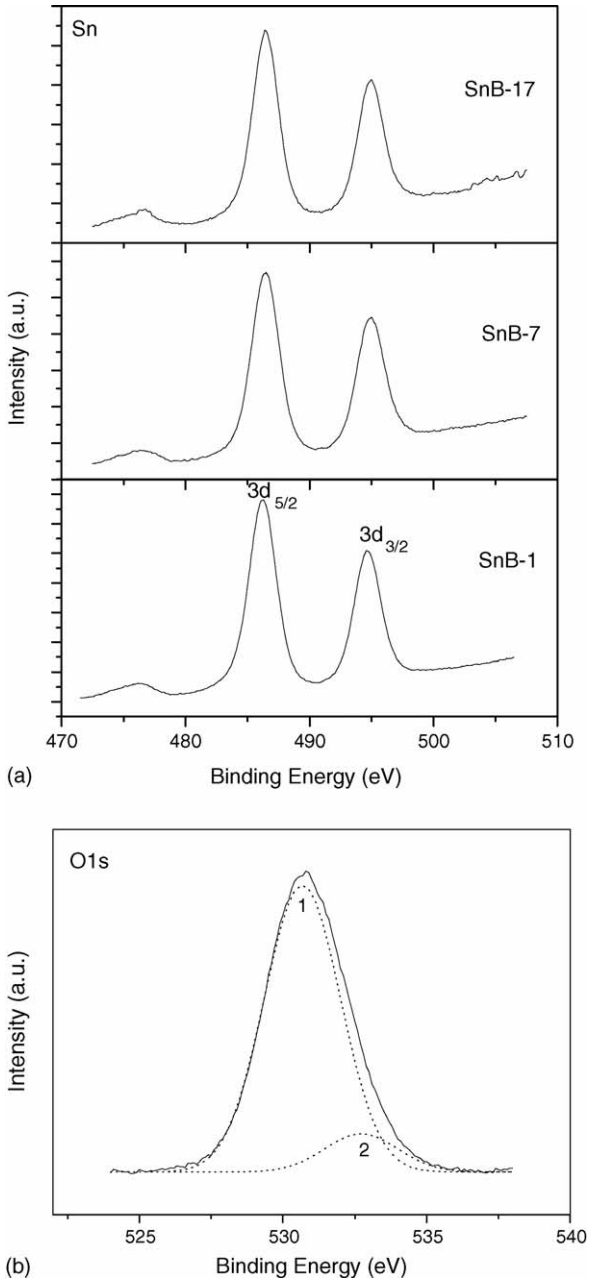

Fig. 3. High resolution XPS of the drug sample showing (a) Sn $3d_{5/2}$, Sn $3d_{3/2}$ and (b) O 1s.

Table 3
Relative surface atomic concentration from XPS data

Sample	Element (at.%)		
	Sn	O	Ca
SNB-1	21.4	74.8	3.6
SNB-7	18.5	79.4	2.1
SNB-17	16.8	81.2	2.0

earlier. This can be further correlated to the nature of the peak for O 1s spectra of 'vanga bhasma' at different cycles of calcinations. A typical XPS spectra is shown in Fig. 3(b) for SNB-1 sample. The broadness of the O 1s peak suggested that different compounds were formed on the surface during the calcination cycle. The subsequent calcination cycles also showed similar shape of the O 1s peak in XPS spectra, except SNB-17 sample. O 1s peaks 1 and 2 could be resolved by using a curve fitting procedure. Peak 1 at a lower energy of 531.1 eV [13] was attributable to oxygen in SnO_2 while peak 2 at higher energy of 532.5–533.0 eV was attributed to oxygen adsorbed/OH species on the surface of SnO_2 of 'vanga bhasma' [13,14]. The probable explanation for these observations is as follows.

During the first calcination, calcium oxide formed from calcium carbonate has strong affinity for water to give $Ca(OH)_2$ through the reaction (1),

$$CaO + H_2O \rightarrow Ca(OH)_2 \quad (1)$$

Simultaneously, the interaction of Sn with the atmospheric oxygen formed various phases namely SnO, SnO_2 and $Ca(OH)_2$, was used up for hydroxylation to form $Sn(OH)_4$, leading to SnO_2 through the reaction (2), [15]

$$Sn(OH)_4 \rightarrow SnO_2 + 2H_2O \quad (2)$$

$Ca(OH)_2$ having strong affinity for CO_2 also formed $Ca(CO)_3$ through the reaction (3), [16]

$$CaCO_3 \rightarrow CaO + CO_2 \quad (3)$$

The presence of carbonate and hydroxyl was also supported by IR studies (Section 3.4).

Another important observation from XPS studies was that the relative surface atomic concentration of Sn decreased as number of calcination cycles increased (Table 3), which was exactly reverse of the EDX analysis (Table 2) where total Sn content was found to increase with the number of calcination cycles. This observation suggests that the Ca ions diffused out on the surface with number of calcination cycles. This caused the particle size stabilization of SnO_2, which was consistent with SEM observation.

For SNB-17 sample, area under the curve for peak 2 was remarkably less as compared to SNB-1 and SNB-7 samples. This indicates that the formation of adsorbed oxygen/OH was less in case of SNB-17 (final product) of 'vanga bhasma' as compared to its intermediate stages. In other words, the extent of formation of SnO_2 was large in SNB-17. Since SnO_2 has a tendency to attract oxygen (negative electron density) due to its Lewis acid sites available [17], the number of calcination cycles

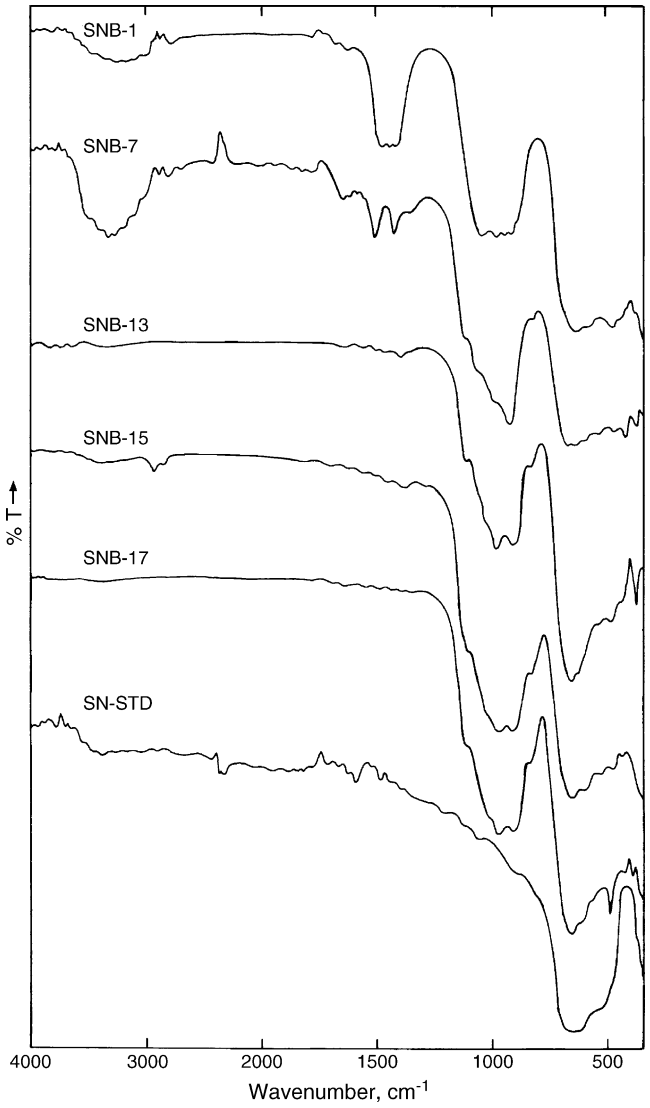

Fig. 4. FT-IR of standard SnO_2 and the drug samples.

increased the oxygen interaction with tin in the 'bhasmikarana' process to form SnO_2 rather than getting adsorbed on the surface of SnO_2. Thus, XPS studies clearly showed that as the number of calcination cycles increased more and more formation of stable SnO_2 took place and thus purity of 'vanga bhasma' also increased.

3.4. Infrared spectroscopy

FT-IR spectra (Fig. 4) of 'vanga bhasma' at different calcination cycles showed strong vibrations in the region of 3265–3270 cm^{-1} for SNB-1 and SNB-7 samples indicating the presence of hydroxyl groups due to formation of tin hydroxide [18,19]. For samples SNB-13 onwards no such peaks were observed in this region indicating the conversion of tin hydroxide into tin (IV) oxide in the subsequent steps. In SNB-1, the peak at 1040 cm^{-1} could be also assigned to tin hydroxide [18], which disappeared in the following cycles of calcination. The weak bands at 1767 and 1641 cm^{-1} (in SNB-1 and SNB-7) could be due to νOH deformation [20] that also disappeared in the latter stages of calcination. The formation of SnO_2 via tin hydroxide could be explained by the reaction (2) given above [15]. Initial formation of tin hydroxide could be due to the trituration of metallic tin with plant juices, which have water as a major constituent. The standard sample of SnO_2 did not show presence of −OH peaks.

In SNB-1 and SNB-7 samples, prominent peaks were observed around 1421 cm^{-1} which were due to CO_3^{-2} [21] from $CaCO_3$. The source of calcium carbonate was tamarind (*Tamarindus indica*) shells, which were used during the trituration procedure, which contain large amount (11.1%) of calcium salt [9]. For samples SNB-13 to SNB-17 no such peaks were observed indicating that $CaCO_3$ was decomposed gradually during subsequent calcination cycles as shown by reaction (3). Additional strong bands were observed around 915–980 cm^{-1} in all the samples and broad nature of the peaks were indicative of overlapping of adjacent peaks due to: (i) adsorbed oxygen species intermediate between O_2^- and O_2^{2-} [22] or Sn–OH [18] and (ii) calcium oxide [21]. Both these possibilities exist since, chemisorbed oxygen species was also evident from XPS studies (mentioned above) and calcium oxide formation could be possible as per the Eq. (3). However, the extent of contribution of either step could not confirmed in the present work. The most dominating peaks in the region of 628–665 cm^{-1} in all samples were attributable to ν(O–Sn–O) bridge functional group in SnO_2 [18,19]. The band position, their shape and intensity were compared with those of the standard SnO_2 confirming that SnO_2 was the major constituent of the 'vanga bhasma'. Other small peaks around 416–553 cm^{-1} and 356–380 cm^{-1} were also due to tin oxide (SnO_2) [18].

Far IR spectra of 'vanga bhasma' at different calcination steps showed a broad band around 315 cm^{-1} in SNB-1 which intensified with number of calcination cycles and was the maximum in SNB-17, which could be assigned to Sn(IV) species from SnO_2 [21]. The significant increase in its (315 cm^{-1}) intensity from SNB-1 to SNB-17 samples indicates the complete oxidation of tin to SnO_2. This again confirms the role of several calcination cycles in the total formation of SnO_2. Two bands at 270 and 155 cm^{-1} were also observed particularly in SNB-15 and SNB-17 samples, which could be assigned to ν(Sn-O) [18].

3.5. Thermogravimetric analysis

From the thermograms of various calcination stages it was observed that there was a significant weight gain (5.83%) in the temperature range 650–820 °C for SNB-1. This weight gain could be due to either oxidation or adsorption of oxygen on the surface of the sample [23]. Availability of Lewis acid sites on SnO_2, after its formation in the first cycle of calcination gives it a great affinity for oxygen showing weight gain during the first calcination. For SNB-7 sample significant weight loss (−5.05%) was observed in the temperature range 880–900 °C which could be attributable partly to: (i) loss of water due to decomposition of $Sn(OH)_4$ [24] and (ii) partly due to decomposition of $CaCO_3$ [25]. For SNB-13 to SNB-17 samples, practically no weight loss/gain was observed in the temperature range of 30–900 °C

indicating that from seventh cycle of calcination cycle $Sn(OH)_4$ was completely converted into SnO_2 and $CaCO_3$ into CaO. Thus, from 13th cycle of calcination onwards 'vanga bhasma' was thermally stable confirming complete formation of SnO_2. While, the standard SnO_2 was found to be moderately stable as a small weight loss was observed due to loss of moisture.

3.6. BET surface area

The specific surface area of the particles of the drug 'vanga bhasma' at different stages of calcination along with that of standard SnO_2 were measured by N_2 desorption. It was found that the specific surface area of SNB-1 was almost half (3.1 m^2/g) of that of the standard SnO_2 (7 m^2/g) and it decreased further to 0.96 m^2/g with increase in number of calcinations up to SNB-15. This was in accordance with the fact that bigger particles were obtained due to the typical preparation method of the drug and agglomeration taking place in repeated calcination stages. This was also evidenced by the SEM results discussed in Section 3.2. However, in case of SNB-17, the surface area increased by about 11% than the previous SNB-15 sample, which supported the SEM result that the particle size of SNB-17 was less than the previous samples. From the results of IR, XPS, TG studies, it was confirmed that as the number of calcination cycles involved in typical traditional method, complete formation of stable SnO_2 took place. Due to the presence of excess chemisorbed oxygen on the surface, an electric double layer was formed around tin oxide, which prevented the agglomeration of the two particles of tin oxide thus giving a stable minimum size of SnO_2.

4. Conclusion

Tin oxide based Ayurvedic drug popularly known as 'vanga bhasma' derived from metallic tin, is among the seven Ayurvedic bhasmas having an important medicinal property for various types of genito-urinary tract disorders. A detailed structural characterization of this drug sample at various stages of calcination was carried out. Based on these results, we proposed a step-wise oxidation of tin going through its hydroxide formation. From XPS studies, it was also confirmed that tin was present in its +4 oxidation state. SEM and XRD results revealed that the particle size of SnO_2 stabilized around 25 nm (due to calcium present), which was lower than that of the standard SnO_2 sample.

Acknowledgement

One of the authors M.P.W. is thankful to CSIR (New Delhi) for the award of Research Associateship.

References

[1] M.P. Wadekar, C.V. Rode, Y.N. Bendale, K.R. Patil, A.A. Prabhune, J. Pharm. Biomed. Anal. 39 (2005) 951–955.
[2] S.B. Kulkarni-Dudhgaonkar, Rasaratnasamuchyaya, Shivaji University Publication, India, 1970.
[3] V. Nagraju, D. Joshi, N.C. Aryya, Ancient Sci. Life 1 (1985) 42–48.
[4] K.M. Nadkarni, Indian Materia Medica, 2, third ed., Bombay Popular Publication, India, 1999, pp. 116–117.
[5] S. Pandit, T.K. Biswas, P.K. Debnath, A.V. Saha, U. Chowdhury, B.P. Shaw, S. Sen, B. Mukharjee, J. Ethnopharmacol. 65 (1999) 149–156.
[6] L. Abello, B. Bochu, A. Gaskov, S. Koudryavtseva, G. Lucazeau, M. Roumyantseva, J. Solid State Chem. 135 (1998) 78–85.
[7] C.H. Shek, J.K.L. Lai, G.M. Lin, Y.F. Zheng, W.H. Liu, Phys. Chem. Solids 58 (1997) 13–17.
[8] H.P. Klug, L.E. Alexander, X-Ray Diffraction Procedures for Polycrystalline and Amorphous Materials, New York, 1974, pp. 618–619.
[9] S.H. Bhosale, Studies in Ayurvedic Inorganic Pharmaceuticals of Plant and Animal Origin, M. Phil Thesis, University of Pune, 1992.
[10] B. Min, S.D. Choi, Sens. Actuators B 99 (2004) 288–296.
[11] J. Calderer, P. Molinas, J. Sueiras, E. Llobet, X. Vilanova, X. Correig, F. Masana, A. Rodriguez, Microelectron. Reliab. 40 (2000) 807–810.
[12] P.Y. Liu, J.F. Chen, W.D. Sun, Vaccum 76 (2004) 7–11.
[13] N. Shirahata, Y. Masuda, T. Yonezawa, K. Koumoto, J. Eur. Ceram. Soc. 24 (2004) 427–434.
[14] T. Kawabe, K. Tabata, E. Szuki, Y. Yamaguchi, Y. Nagasava, J. Phys. Chem. 105 (2001) 4239–4244.
[15] E.W. Giesekke, H.S. Gutowsky, P. Kirkov, H.A. Laitenen, Inorg. Chem. 6 (1967) 1294–1297.
[16] J. Huang, K.E. Daugherty, Thermochim. Acta 118 (1987) 135–141.
[17] F.A. Cotton, Wilkinson, Advanced Inorganic Chemistry, third ed., Wiley Eastern Ltd., 1972, pp. 326–327.
[18] D. Amalric-Popescu, F. Bozon-Veduraz, Catal. Today 70 (2001) 139–154.
[19] J. Zhang, L. Gao, J. Solid State Chem. 177 (2004) 1425–1430.
[20] N. Sergent, P. Gelin, L. Perier-Camby, H. Praliaud, G. Thomas, Sens. Actuators B 84 (2002) 176–188.
[21] R.A. Nyquist, R.O. Kagel, Infrared Spectra of Inorganic Compounds, Academic press, New York, London, 1971, pp. 220–221.
[22] T.A. Gudrizer, A.A. Davydov, React. Kinet. Catal. Lett. 3 (1975) 63–67.
[23] W.W. Wendlandt, Thermal Analysis, third ed., Wiley-Interscience, 1986, p. 14,139.
[24] F. Liu, B. Quan, Z. Liu, L. Chen, Mater. Chem. Phys. 93 (2005) 301–304.
[25] S. Ghardashkhani, D.A. Cooper, Thermochim. Acta 161 (1990) 327–337.